

# Highly Sensitive and Multiplexed Detection of Low-Frequency Mutation in Fragmented ctDNA by a Dual-Role Mediator Blocker Amplification Strategy

Rui Zhang,<sup>▽</sup> Zhening Pu,<sup>▽</sup> Daxing Xu, Ying Yin, Bingbing Wei,<sup>\*</sup> Lei Wang,<sup>\*</sup> and Zhaocheng Liu<sup>\*</sup>



Cite This: *Anal. Chem.* 2025, 97, 22407–22417



Read Online

ACCESS |



Metrics & More

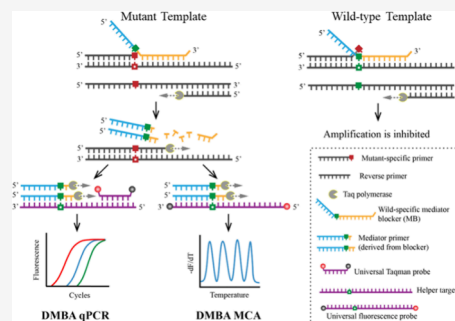


Article Recommendations



Supporting Information

**ABSTRACT:** The detection of mutations in circulating tumor DNA (ctDNA) is challenging due to the significant fragmentation of ctDNA and the high prevalence of the wild-type template. Additionally, variant detection through qPCR is typically dependent on target-specific fluorescence probes, and no more than five targets can be identified in a single reaction due to the limited fluorescence colors in thermal cyclers. To address these limitations, we introduce the Dual-Role Mediator Blocker Amplification (DMBA) strategy, enabling sensitive and multiplex mutation detection without reliance on specific fluorescence probes. This strategy is applicable in both qPCR and melting curve analysis (MCA) platforms. The mediator blockers in DMBA play dual roles: enhancing discrimination between wild-type and mutant DNA and releasing mediator primers. These mediator primers extend the helper target and cleave universal fluorescence probes in qPCR, enabling the detection of mutations at variant allele fractions (VAFs) as low as 0.01%. The DMBA MCA method can identify multiple mutations, overcoming limitations in fluorescence channels by using mediator primers to extend universal fluorescence probes, producing fluorescent double strands with different  $T_m$ 's and colors. Multiplexed DMBA-MCA was developed to detect seven variants at 0.1–0.5% VAF in one tube. Our innovative method offers advantages including exceptional sensitivity, elimination of the requirement for specific fluorescence probes, shorter amplicons, and high multiplexing capacity, potentially revolutionizing clinical practice and precision medicine.



## INTRODUCTION

Histopathological biopsy remains the clinical gold standard for tumor diagnosis, yet its invasive procedure and limited capacity to overcome tumor heterogeneity restrict comprehensive characterization of dynamic tumor profiles. The advent of liquid biopsy (LB) has revolutionized oncological practice through noninvasive monitoring of circulating biomarkers, including circulating tumor cells (CTCs), circulating tumor DNA (ctDNA), and exosomes, in peripheral blood, enabling early detection, treatment evaluation, and recurrence surveillance.<sup>1–4</sup> Among these biomarkers, ctDNA has garnered particular attention due to its enhanced accessibility, reduced spatial heterogeneity, and tumor-specific genetic signatures.<sup>1,5</sup> The mutational landscape of ctDNA offers clinical utility in therapy guidance, minimal residual disease detection, and population cancer screening.<sup>5–7</sup>

Current ctDNA detection platforms encompass PCR-based approaches,<sup>8–12</sup> next-generation sequencing (NGS),<sup>13–15</sup> and electrochemical biosensors.<sup>16–18</sup> PCR technology, notable for its operational simplicity and adaptability, has evolved into diverse formats for variant detection: amplification-refractory mutation system (ARMS),<sup>8,19</sup> allele-specific blocker PCR (ASB-PCR),<sup>20,21</sup> hairpin competition amplification (HCA),<sup>10</sup> blocker displacement amplification (BDA),<sup>9,22,23</sup> PNA clamping PCR,<sup>24</sup> and coamplification-at-lower denaturation-temper-

ature PCR (COLD-PCR).<sup>25,26</sup> However, these methods face critical limitations in detecting low-abundance mutations due to excessive ctDNA fragmentation and background wild-type DNA interference.

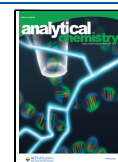
In ARMS, the amplification of mutant DNA was achieved through the use of primers featuring mutant-specific 3' nucleotides.<sup>8,19</sup> Nonetheless, mismatches between the 3' nucleotide of the primer and wild-type DNA occur due to minimal thermodynamic disparities resulting from a single nucleotide change. This leads to significant nonspecific amplification, impeding the ability to detect low-frequency variants. In our recent study, we introduced the unmodified-blocker cleavage PCR (UBC-PCR) technique, employing wild-specific blocker, to enhance the detection of DNA mutations with exceptional sensitivity down to 0.01% variant allele fraction (VAF).<sup>27</sup> While the use of blockers and Taqman probes extends PCR amplicons to a minimum of about 100 bp and sometimes even longer than 150 bp, long amplicons can

**Received:** August 15, 2025

**Revised:** September 20, 2025

**Accepted:** September 22, 2025

**Published:** October 3, 2025





these primers contained one or two template-specific nucleotides at the 3' end.<sup>33</sup> Second, the employment of chemical-modified mediator probes in MeltArray led to increased costs. Lastly, MeltArray was limited to detecting mutations with Variant Allele Frequencies (VAFs) of 5% or 10%, rendering it unable to identify low-frequency mutant DNA.

To tackle these challenges, we introduce the Dual-Role Mediator Blocker Amplification (DMBA; Figure 1) strategy to identify low-frequency mutations using universal fluorescence probes. This strategy employs mediator blockers to (1) enhance wild-type/mutant discrimination; (2) generate mediator primers for either universal probe cleavage (qPCR mode) or fluorescent double-strand production (MCA). It also excludes the specific Taqman probes from the targeted sequence results in shorter amplicons and reduces cost. When combined with MCA, multiple variants can be detected in a single tube through the generation of fluorescent double strands with varying  $T_m$ 's and colors. With its novel reaction mechanism for variant identification, the DMBA platform demonstrates four key advantages: high sensitivity, specific probe-independent detection, short-amplicon, and high-multiplexing, collectively advancing ctDNA analysis for precision oncology applications.

## MATERIALS AND METHODS

**DNA Synthesis.** DNA strands and mutant plasmid templates were synthesized and purified in Genwizhi (Suzhou, China). Mutant plasmid DNA or genomic DNA were spiked into wildtype 293T genomic DNA when used as templates. Concentrations of genomic DNA and plasmid DNA were determined using DeNovix DS-11 Spectrophotometer (DeNovix Inc., Wilmington, DE, USA) and verified by qPCR. Gene-specific primers, blockers, and probes are presented in Supplementary Table S1.

**DNA Extracted from Cultivated Cells, Tissue, and Plasma.** Genomic DNA from BHT101, HCT116, H1299, and 293T cell lines was extracted using the Universal Genomic DNA Kit (CWbio, Jiangsu, China) following the manufacturer's instructions. The BHT101 DNA contained heterogeneous BRAF V600E mutations, while the HCT116 DNA harbored heterogeneous PIK3CA H1047R mutations and H1299 DNA harbored heterogeneous NRAS Q61K mutations with 293T DNA serving as the wild-type control. DNA concentration was quantified using the DeNovix DS-11 Spectrophotometer (DeNovix Inc., Wilmington, DE, USA) and normalized by qPCR. Genomic DNA from fine-needle aspiration (FNA) samples of thyroid cancer patients was isolated using the same Universal Genomic DNA Kit (CWbio, Jiangsu, China). Cell-free circulating tumor DNA (ctDNA) was extracted from 3 mL of plasma from lung cancer patients using the AmoyDx cell-free DNA extraction kit.<sup>34</sup> Following the manufacturers' instructions, Buffer CDL, Digest Solution, prechilled isopropanol, Buffer CDB, Buffer CDD, anhydrous ethanol, Buffer CW1, Buffer CW2, and Buffer CDE were sequentially utilized alongside vortexing and centrifugation steps. The extracted DNA is subsequently stored at temperatures below  $-20\text{ }^{\circ}\text{C}$  for future use.

**qPCR Experiments.** All real-time PCR assays were performed on a SLAN-96S Real-Time PCR system (Hongshi Medical Technology, Shanghai, China) in a 30  $\mu\text{L}$  volume. All the assays were performed in triplicates containing 0.03 U/ $\mu\text{L}$  Taq polymerase (TransGen, Beijing, China), 1.6–2.5 mM

$\text{Mg}^{2+}$ , 0.2  $\mu\text{M}$  dNTPs, and 10  $\mu\text{L}$  templates under reaction conditions of 95  $^{\circ}\text{C}$  for 3 min, followed by 55 cycles of 95  $^{\circ}\text{C}$  for 10 s, annealing/extending at 56 or 59  $^{\circ}\text{C}$  for 15 s, and fluorescence collection at 74  $^{\circ}\text{C}$  for 20 s, unless specified otherwise. Different samples with a variety of variant allele fractions (VAFs) at proportions of 50%, 10%, 1%, 0.1%, 0.01%, or 0% by mixing the mutant DNA and wild-type DNA (30 ng/ $\mu\text{L}$  293T genomic DNA) were examined.

Duplex assays were performed with 0.04 U/ $\mu\text{L}$  Taq polymerase (TransGen, Beijing, China), 2.5 mM  $\text{Mg}^{2+}$ , and 0.2  $\mu\text{M}$  dNTPs under reaction conditions of 95  $^{\circ}\text{C}$  for 15 min, followed by 55 cycles of 95  $^{\circ}\text{C}$  for 10 s of annealing/extending at 56 or 59  $^{\circ}\text{C}$  for 15 s and fluorescence collection at 74  $^{\circ}\text{C}$  for 20 s.  $\Delta\text{Ct}$  cutoff values for each mutant was determined by subtracting the Ct value of the 0% VAF sample from Ct values of the reference (Cut-off value =  $\text{Ct}[0\% \text{ VAF sample}] - \text{Ct}[\text{reference}] - 3 \times \text{SD}[0\% \text{ VAF sample}]$ ). If no amplification signal was detected, the Ct value for a sample with 0% VAF was set at 55 with a standard deviation of 2. If  $\Delta\text{Ct}$  was less than the cutoff value, the sample was classified as positive; if  $\Delta\text{Ct}$  was greater than the cutoff value, the sample was classified as negative or below the limit of detection. Amounts of primers, blockers, and probes used in the qPCR assays are presented in Supplementary Table S2.

**ddPCR Assay Targeting EGFR L858R Mutation.** The ddPCR assay was performed on a AD3200 Droplet Digital PCR System<sup>35</sup> (Pilot, Zhejiang, China). A total of 15  $\mu\text{L}$  of reaction Master Mix containing 3  $\mu\text{L}$  of ddPCR Supermix, 1  $\mu\text{M}$  primer, 0.3  $\mu\text{M}$  Taqman probes, and 5  $\mu\text{L}$  of ctDNA sample was prepared and loaded onto the reaction cartridges for droplet generation. Then, the thermal cycling step started with 10 min at 95  $^{\circ}\text{C}$ , followed by 50 cycles of 30 s at 95  $^{\circ}\text{C}$  for DNA denaturation and 1 min at 60  $^{\circ}\text{C}$  for annealing/extension. After PCR, the plate was loaded onto an AD3200 Reader (Pilot, Zhejiang, China) to collect droplet fluorescence data.

**Mutation Detection by MCA Assay.** All MCA assays were performed on an SLAN-96S Real-Time PCR system (Hongshi Medical Technology, Shanghai, China) in a 30  $\mu\text{L}$  volume. The MCA assay was performed in triplicates containing 0.03 U/ $\mu\text{L}$  Taq polymerase (TransGen, Beijing, China), 2 mM  $\text{Mg}^{2+}$ , 0.2  $\mu\text{M}$  dNTPs, and 10  $\mu\text{L}$  templates under reaction conditions of 95  $^{\circ}\text{C}$  for 3 min, 55 cycles of 95  $^{\circ}\text{C}$  for 10 s, annealing at 58  $^{\circ}\text{C}$  for 15 s, and extending at 72  $^{\circ}\text{C}$  for 10 s and then 45  $^{\circ}\text{C}$  for 5 min, 95  $^{\circ}\text{C}$  for 10 s, and 50  $^{\circ}\text{C}$  for 2 min, followed by a temperature increase from 50 to 90  $^{\circ}\text{C}$  (0.04  $^{\circ}\text{C}/\text{step}$ ). Fluorescence data were measured at each step of the continuous temperature increase during the melting curve analysis procedure. Different samples with a variety of variant allele fractions (VAFs) at proportions of 50%, 10%, 1%, 0.1%, 0.03%, or 0% by mixing the mutant DNA and wild-type DNA (30 ng/ $\mu\text{L}$  293T genomic DNA) were examined.

The multiplexed DMBA MCA assay was performed with 0.06 U/ $\mu\text{L}$  Taq polymerase (TransGen, Beijing, China) and 4.5 mM  $\text{Mg}^{2+}$ , 0.25  $\mu\text{M}$  dNTPs, and 10  $\mu\text{L}$  templates in a 30  $\mu\text{L}$  volume. The protocol mirrored the aforementioned steps with the exception of annealing at 58  $^{\circ}\text{C}$  for 20 s. Different samples with a variety of variant allele fractions (VAFs) of 10%, 1%, 0.5%, 0.3%, 0.1%, or 0% by mixing the mutant DNA and wild-type DNA (30 ng/ $\mu\text{L}$  293T genomic DNA) were examined. Amounts of primers, blockers, and probes used in MCA assays are presented in Supplementary Table S3.



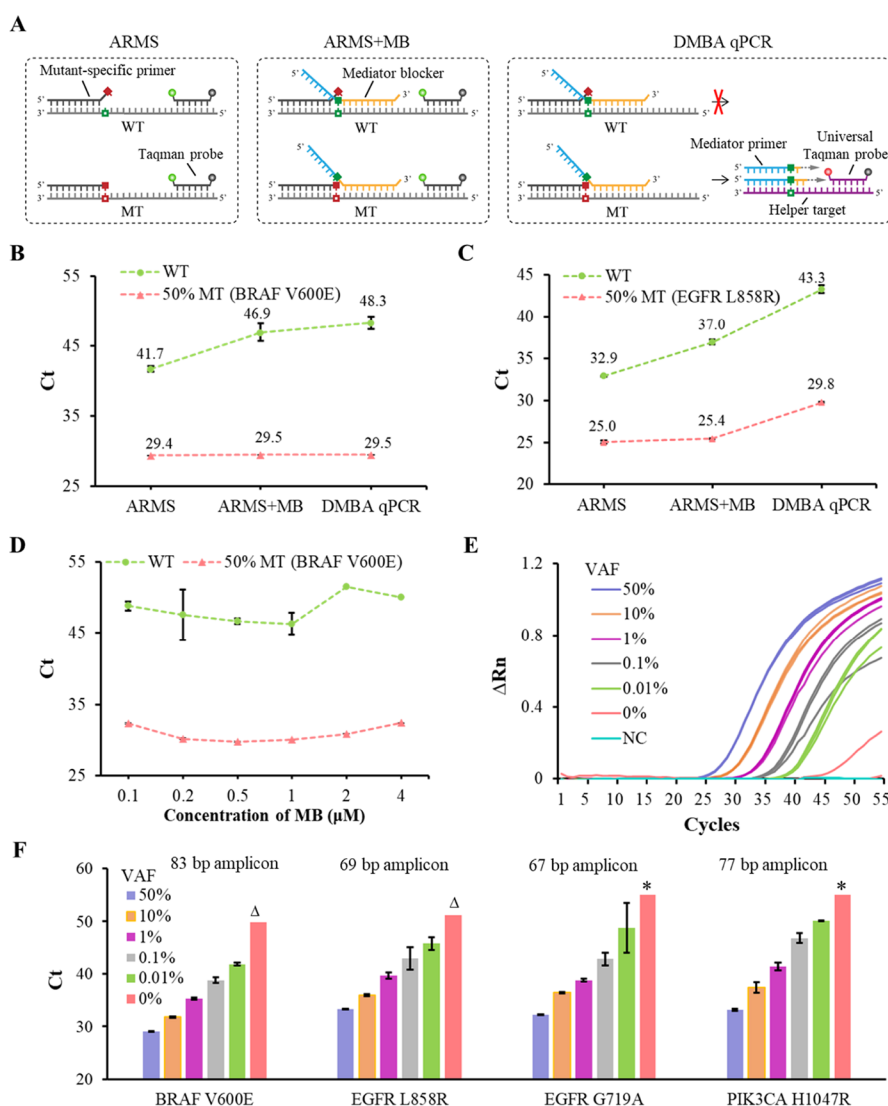


**Figure 2.** Development of DMBA qPCR. (A) Examining the impact of mediator blockers on mutation detection by formulating three comparative assays. (B) Different methods were employed to amplify WT and 50% MT (BRAF V600E mutation). The error bars indicate the standard deviation of triplicate determinations across all assays. (C) Different methods were employed to detect the EGFR L858R mutation. (D) Varying amounts of mediator blockers were tested in DRMB qPCR targeting the BRAF V600E mutation. (E) Amplified traces of the BRAF V600E variant at different VAFs are presented. These different VAF samples were prepared by spiking mutant DNA into wild-type DNA (30 ng/ $\mu$ L 293T genomic DNA). For example, the 1% VAF samples contained 900 mutant DNA copies and 89100 wildtype DNA copies. (F) Summary of Ct values and amplicons' length targeting BRAF V600E, EGFR L858R, G719A, and PIK3CA H1047R are shown. The asterisk (\*) denotes the absence of signal, with Ct values set to 55. Only one of the triplicates showed a signal, which was indicated by a triangle ( $\Delta$ ). Error bars indicate the standard deviation of triplicate measurements.

## RESULTS

**Overview of DMBA qPCR and MCA.** This study presents a novel strategy for detecting low-frequency mutant DNA using universal fluorescence probes in qPCR and the melting curve analysis (MCA) technique (Figure 1). Our methodology involves the use of mutant-specific primers, similar to those in ARMS with mutant-specific 3' nucleotide,<sup>8,19</sup> along with wild-specific mediator blockers (MBs). The wild-specific MBs comprise three regions: a 5' sequence (blue), a middle sequence (yellow), and a 3' end tail. The 5' sequence serves as the main region of the mediator primers. The middle sequence binds to the templates with its 5' end specifically designed to match the wildtype nucleotide. We included a four-nucleotide unpaired tail at the 3' end of the mediator blockers to inhibit

extension, a strategy shown to be effective in our previous research.<sup>27,33</sup>

The MBs are typically designed with a higher  $T_m$  than the mutant-specific primers to enable thermodynamically favorable hybridization to templates. Both MBs and mutant-specific primers bind to the mutant template (MT) during amplification. The 5' nucleotide of MBs' middle sequence unbinds with the mutant nucleotide, while the 3' end of mutant-specific primers perfectly match with the MT, thereby ensuring smooth initiation of extension. During this process, MBs are cleaved by Taq polymerase to produce mediator primers with wild-specific nucleotide plus one or two template-specific nucleotides (highlighted in yellow) at the 3' terminus.<sup>33</sup> Subsequently, the mediator primers bind to the helper target and are extended by the Taq polymerase, leading to the hydrolysis of universal fluorescence probes in qPCR.

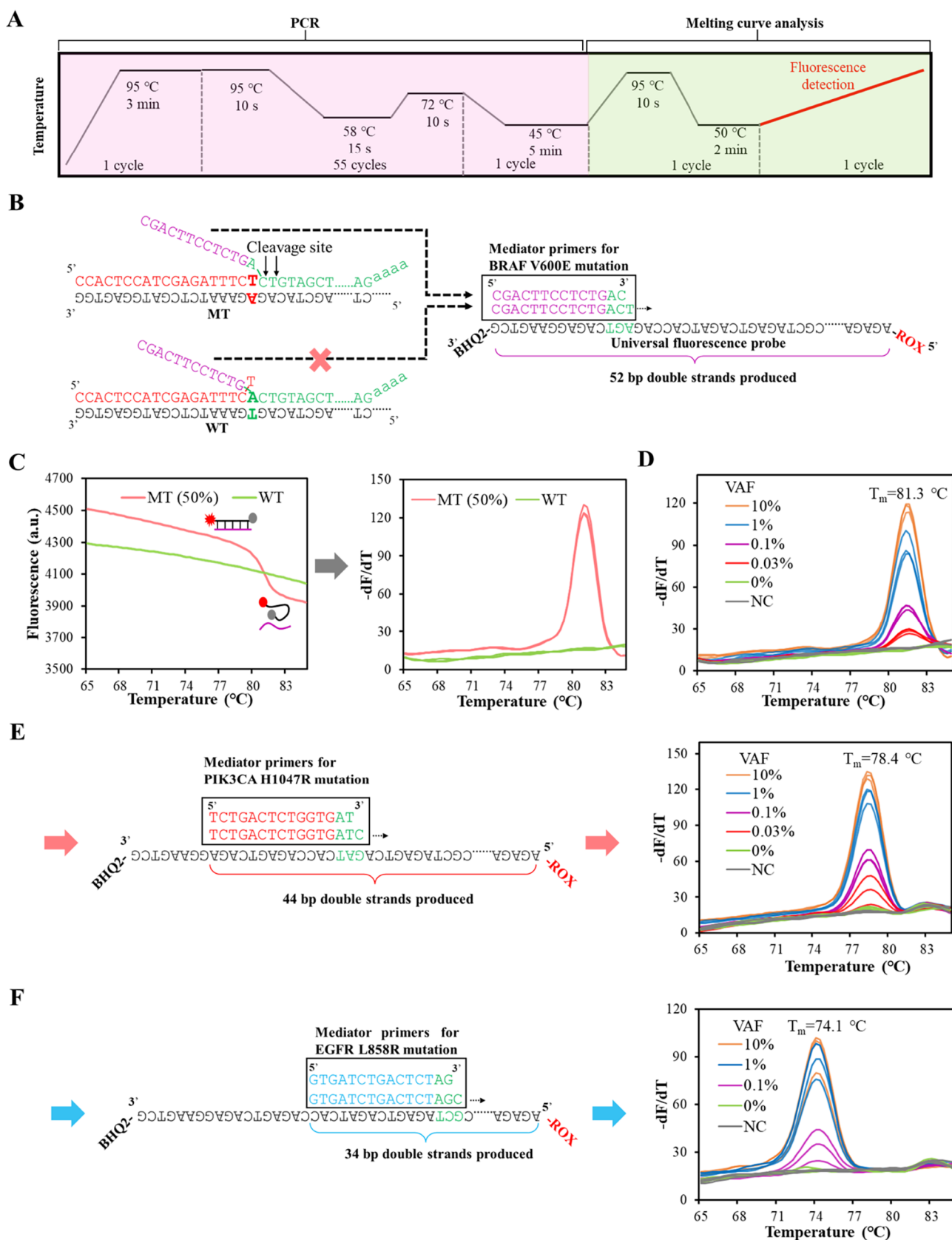


**Figure 3.** Mutation identification by DMBA MCA. (A) The reaction process of DMBA MCA comprises PCR and melting curve analysis. (B) Sequence of mediator blocker (highlighted in purple and green), mutant primer (highlighted in red), mediator primers and universal fluorescence probe used in DMBA MCA for BRAF V600E mutation detection. Mediator primers extend the universal fluorescence probe and generate 52 bp fluorescent double strands. (C) Fluorescent double-strand transition into random coils as temperature gradually increases, leading to a significant decrease in fluorescence intensity and the appearance of a distinct melting peak. (D) Mutant DNA at various VAFs were tested by DMBA MCA,

Figure 3. continued

showing the sensitivity of 0.03% VAF. (E) DMBA MCA was developed for PIK3CA H1047R. (F) DMBA MCA targeting EGFR L858R was established.

MT undergoes exponential amplification with the mediator primers produced and fluorescence accumulation in each qPCR cycle. In contrast, the wild-type template (WT) is bound by wild-specific MBs, preventing the 3' end of mutant-specific primers from pairing with the template further. This inhibition effectively suppresses WT amplification and reduces the level of mediator primer production.

In addition to qPCR, the novel approach can be integrated with melting curve analysis (MCA). During MCA, mediator primers released from MBs bind to a universal fluorescence probe and are extended, producing double fluorescent double strands. As the temperature rises in MCA, these double strands dissociate, generating observable melting peaks at specific temperatures ( $T_m$  values). To precisely identify mutant DNA, it is essential to optimize the MBs to inhibit mediator primer production or eliminate melting peaks in WT amplification. Binding to different regions of a universal fluorescence probe can produce fluorescent double strands with varying lengths ( $T_m$  values). The capacity to detect multiple targets in a single reaction is expanded by employing multiple fluorescence probes with distinct colors. Therefore, the simultaneous detection of numerous mutations is achieved by generating fluorescent double strands with different lengths ( $T_m$  values) and colors specific to various mutation targets.

The MBs in this strategy have dual essential functions: improving discrimination between wild-type and mutant DNA and producing mediator primers to initiate the hydrolysis of universal fluorescence probes or produce fluorescent double strands. This method, termed dual-role mediator blocker amplification (DMBA), provides advantages including enhanced sensitivity, short amplicon size, multiplexed variant detection, and cost-effectiveness.

**Development of DMBA qPCR.** To exhibit the discrimination ability using mediator blockers and universal fluorescence probes, three different assays were designed and performed (Figure 2A). ARMS is based on the use of primers whose 3' nucleotides are mutant-specific.<sup>8,19</sup> In the ARMS +MB assay, mediator blockers were employed in conjunction with mutant-specific primers and a template-specific Taqman probe. DMBA qPCR applied mediator blockers, universal Taqman probe, and helper target. First,  $\Delta C_t$  values between wild and 50% BRAF V600E mutant DNA was 12.3 when using mutant-specific primers (Figure 2B), while the addition of mediator blockers enhanced the  $\Delta C_t$  values from 12.3 to 17.4, demonstrating that the mediator blockers increased the discrimination ability of reaction (Figure 2B). Next,  $\Delta C_t$  values remain as large as 18.8 when using a universal fluorescence probe and helper target to replace a specific Taqman probe (Figure 2B). A similar result was achieved targeting EGFR L858R mutation (Figure 2C). The results demonstrate that DMBA qPCR can effectively detect mutant DNA with enhanced discrimination despite the use of a universal fluorescence probe. Next, varying amounts of mediator blockers were tested in DRMB qPCR targeting the BRAF V600E mutation (Figure 2D). Inadequate use of mediator blockers at a concentration of 0.1  $\mu$ M resulted in reduced  $\Delta R_n$  and  $C_t$  value delays (Figure 2D, Supplementary Figure S1A). This is because insufficient mediator blockers

lead to inadequate mediator primer generation. Conversely, excessive mediator blockers at 4  $\mu$ M also caused  $C_t$  delays, indicating significant inhibition in amplifying both WT and MT (Figure 2D, Supplementary Figure S1B). The optimal mediator blockers should effectively inhibit WT amplification without substantially reducing MT amplification.

According to the established guidelines for developing DMBA, assays targeting different mutations were established, and their sensitivity was assessed individually. Amplification curves detecting the BRAF V600E variant showed the ability to discriminate mutant DNA at a VAF of as little as 0.01% using DRMB PCR (Figure 2E). Additionally, assays targeting EGFR L858R, G719A, and PIK3CA H1047R were developed using the same universal fluorescence probe. Akin to the BRAF V600E variant assays, all discrimination assays achieved a sensitivity of 0.01% VAF (Figure 2F), demonstrating remarkable sensitivity. The elimination of specific fluorescence probes reduced costs and shortened amplicons to lengths between 67 and 83 bp (Figure 2F), offering advantages for amplifying fragmented ctDNA.

**Investigation of DMBA MCA for Mutation Identification.** In addition to its application with qPCR, DMBA can also be utilized for mutation identification in combination with the melting curve analysis (MCA) technique (Figure 3A). Illustrated in Figure 3B is the application of DMBA MCA for identifying the BRAF V600E mutation. Mediator primers are only produced during amplification of the mutant template (MT) by a mutant-specific primer. These mediator primers then extend the fluorescence probe, resulting in the formation of double-stranded fluorescent products. Conversely, in wild-type (WT) amplification, there is minimal production of mediator primers or double-stranded products due to the inability of mutant-specific primers to bind to the WT sequence in the presence of wild-type mediator blockers (Figure 3B). During the melting analysis, the fluorescent double-strand transition into random coils with increasing temperature, leading to a significant decrease in fluorescence intensity and the appearance of a distinct melting peak (Figure 3C). In contrast, the amplification of the WT sequence does not exhibit a melting peak as the generation of mediator primers and double strands is effectively inhibited by the mediator blockers (Figure 3C).

Next, the mutant DNA at various VAFs was assessed using the optimized DMBA MCA to determine its sensitivity. The analysis revealed the capability of DMBA MCA to detect mutant DNA at levels as low as 0.03% VAF, indicating its high sensitivity (Figure 3D). Additionally, assays were developed for PIK3CA H1047R and EGFR L858R mutation using the universal fluorescence probe (Figure 3E,F). Mutant DNA at levels as low as 0.03% and 0.1% VAFs could be distinguished, respectively. Optimizing the length and quantity of mediator blockers was crucial for achieving highly sensitive and specific mutation detection (Supplementary Figure S2). An effective mediator blocker should inhibit the production of double-stranded species in WT amplification while not impeding the production of double-stranded species in MT amplification. The melting peaks for three mutations displayed distinct  $T_m$  values of 81.3, 78.4, and 74.1  $^{\circ}$ C due to the different lengths of

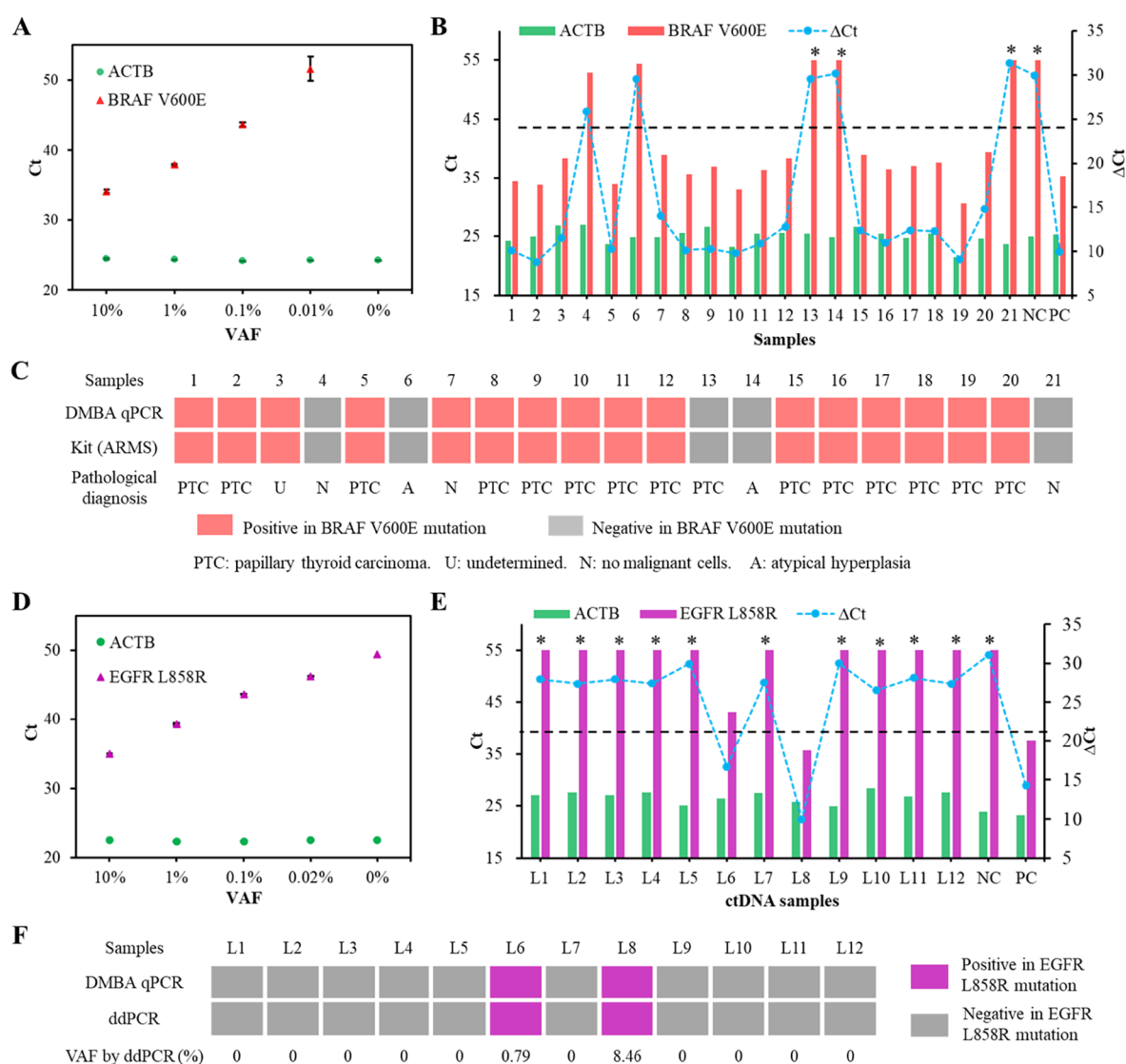


**Figure 4.** Identification of mutation in FNA DNA and ctDNA samples using DMBA qPCR. (A) A duplex assay was developed to target the BRAF V600E mutation and ACTB. The error bars in the figures represent the standard deviation of triplicate determinations. (B) Ct values were obtained for the BRAF V600E mutation and a reference target in the examination of 21 FNA DNA samples, along with positive control (PC) and negative control (NC). The  $\Delta$ Ct cutoff value for the BRAF V600E mutation was set at 24.7, with a Ct value of 55 assigned in instances where no signal was detected (\*). (C) Summary of the gene status in 21 FNA DNA samples obtained by DMBA qPCR and a commercial kit. (D) A duplex assay was developed to target the EGFR L858R mutation and ACTB. Error bars indicate standard deviation from triplicate determinations. (E) The summary of Ct values for the EGFR L858R mutation and the reference target in 12 ctDNA samples, along with positive control (PC) and negative control (NC), was provided. A dashed line was utilized to indicate the  $\Delta$ Ct cutoff value (20.9) for the EGFR L858R mutation. Instances where no signal was detected were marked with an asterisk (\*), and Ct values of 55 were assigned in these instances. (F) Summary of the gene status in 12 ctDNA samples acquired through DMBA qPCR and ddPCR.

double strands produced (Figure 3D–F). It indicates that DMBA MCA has the potential to detect various mutations in one tube by generating fluorescent double strands with different  $T_m$ 's and colors.

**Detection of Mutation in Clinical Samples by DMBA qPCR.** We developed a duplex assay that combines the DMBA qPCR assay targeting the BRAF V600E mutation with specific Taqman probe qPCR targeting ACTB (reference gene). The sensitivity of the duplex assay for detecting the BRAF V600E mutation was evaluated, demonstrating the ability to detect as little as 0.01% VAF mutant DNA (Figure 4A). Subsequently, 21 FNA (fine needle aspiration) DNA samples from thyroid cancer patients were analyzed using the developed DMBA qPCR. The Ct values for the BRAF V600E mutation and the

reference target were summarized in Figure 4B. According to  $\Delta$ Ct values and the calculated cut off value at 24.7, 16 samples were identified as positive for BRAF V600E mutation, while 5 samples were negative (Figure 4C). Among the 21 patients, 15 were diagnosed with PTC by pathology, and one sample with an undetermined diagnosis by pathology was found to be positive for the BRAF V600E mutation, indicating the diagnostic value of molecular testing. Furthermore, the results showed 100% concordance with those obtained from a commercial kit used in clinical testing (Figure 4C), highlighting the excellent performance of the DMBA qPCR in analyzing gene status from tissue DNA.

Next, another duplex assay was developed to target the EGFR L858R mutation (DMBA qPCR) and ACTB (specific



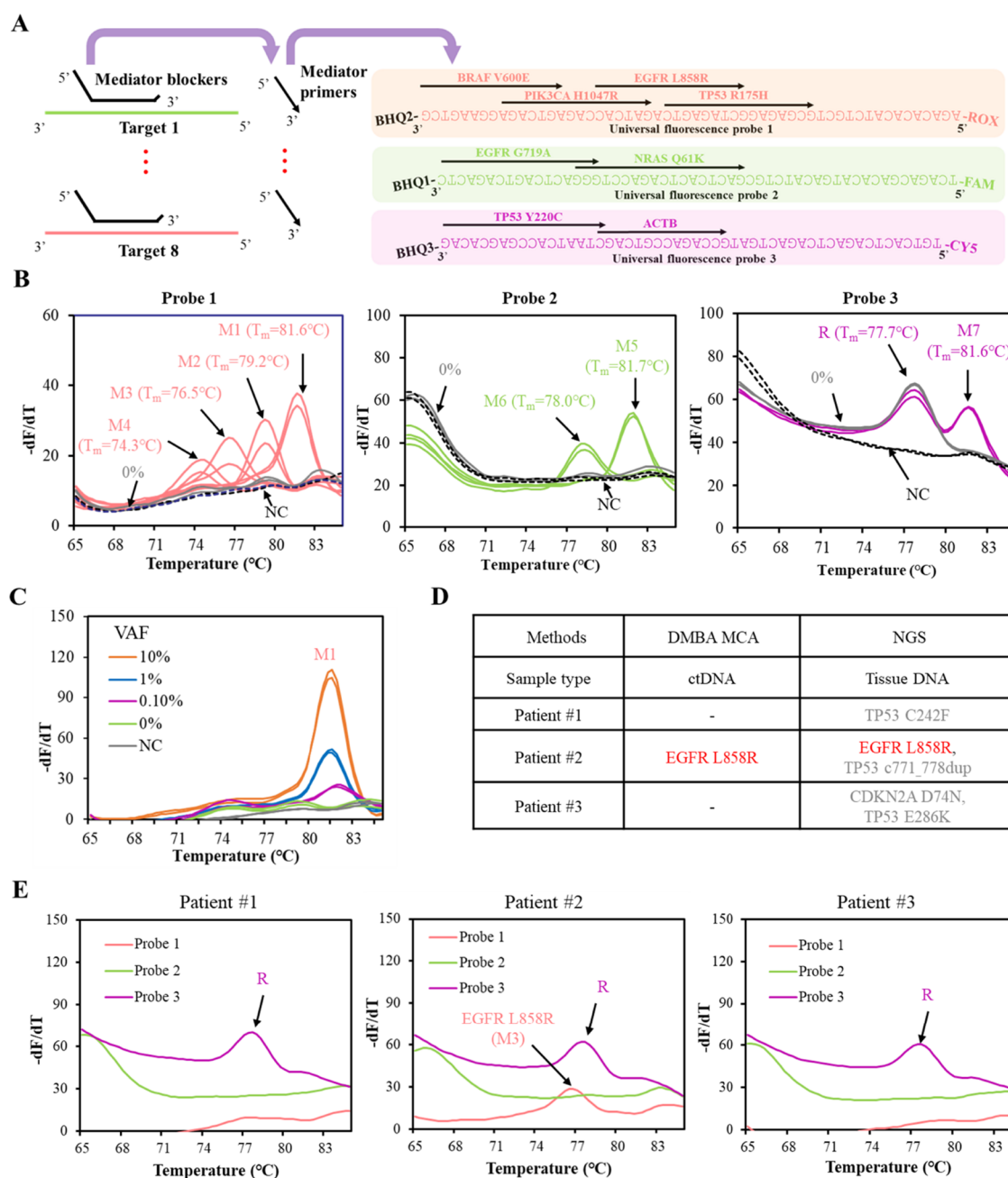


**Figure 5.** Development of a multiplexed DMBA MCA for identifying variants in ctDNA samples. (A) Sequence of universal fluorescence probes and mediator primers for seven mutations and one reference gene in the multiplexed DMBA MCA. Mutation targets were designated as M1 to M7 with ACTB denoted as R. (B) Melting curves of multiplexed DMBA MCA in detecting different mutations of 1% VAF and the reference gene. The samples with a 1% VAF harbored 900 mutant DNA copies and 89,100 wildtype DNA copies.  $T_m$  values for the peaks corresponding to different targets were also provided within brackets. Gray lines depict the curves of wildtype DNA (0% VAF), whereas black dotted lines represent the curves of the no template control (NC). (C) BRAF V600E mutations of different frequencies were tested by multiplexed DMBA MCA as an example. (D) Comparison of detection results from the multiplexed DMBA MCA and NGS. (E) Three ctDNA samples were tested by multiplexed DMBA MCA.

Taqman probes qPCR). The assay successfully detected mutant DNA at levels as low as 0.02% VAF (Figure 4D). Subsequently, 12 plasma ctDNA samples from lung cancer patients were analyzed using this assay. Analysis of Ct values for the EGFR L858R mutation and the reference target is presented in Figure 4E. Two samples tested positive for the EGFR L858R mutation, while ten samples tested negative based on  $\Delta C_t$  values and a calculated cutoff value (Figure 4E). Importantly, the results exhibited 100% concordance with those obtained from ddPCR (Figure 4F), underscoring the

robust performance of DMBA qPCR in analyzing the gene status from plasma ctDNA.

**Detection of Seven Mutations in Plasma ctDNA Samples through Multiplexed DMBA MCA.** By producing and analyzing fluorescent double strands with different  $T_m$ 's and colors, DMBA MCA had the potential of detecting various mutations, more than the numbers of instrument's fluorescence channels. As a proof of concept, one multiplexed DMBA MCA assay was developed to target seven variants and a reference gene, employing three universal fluorescence probes.



Table 1. Comparison of Methods for Mutation Identification

Methods	Platform	Multiplicity	Specific Fluorescence Reporter	Modified/Special Oligo	Tube-opening	Sensitivity
ARMS <sup>8,19</sup>	qPCR	Low	Yes	No	No	1%
ASB-PCR <sup>20</sup>	qPCR	Low	Yes	Yes	No	0.1%
BDA <sup>9,22,23</sup>	qPCR	Low	Yes	No	No	0.01–0.1%
MeltArray <sup>32</sup>	MCA	Moderate	No	Yes	No	5–10%
ddPCR <sup>36,37</sup>	ddPCR	Low	Yes	No	No	0.05%, 0.01%
CRISPR-based approaches <sup>38,39</sup>	CRISPR-Cas12a	Low	No	Yes	Yes	0.01%, 0.002%
CAPP-Seq, <sup>13</sup> SignateraTM <sup>15</sup>	NGS	High			Yes	0.02%, 0.01–0.02%
DMBA in this work	qPCR, MCA	Moderate	No	No	No	0.01–0.1%

The sequences of the universal fluorescence probes and the binding sites of the mediator primers for the different targets are provided (Figure 5A). Probe 1 was designed to target BRAF V600E, PIK3CA H1047R, EGFR L858R, and TP53 R175H mutations. Probe 2 focused on EGFR G719A and NRAS Q61K mutations, while probe 3 was designed for the TP53 Y220C mutation and ACTB (reference gene). The melting curves and  $T_m$  values of the targets are depicted in Figure 5B using mutant DNA samples at 1% VAF. Notably, the 0% VAF sample and the negative control (NC) exhibited no nonspecific melting peaks, underscoring the high specificity of the multiplexed DMBA MCA. Subsequently, the discrimination ability of the multiplexed DMBA MCA was assessed. The assay targeting the BRAF V600E mutation is shown in Figure 5C, and other mutations are presented in Supplementary Figure S3. The results showed multiplexed DMBA MCA had the capability to detect mutant DNA at VAFs of 0.1%, 0.3%, or 0.5% for all seven mutations.

Furthermore, multiplexed DMBA MCA was employed to analyze three ctDNA samples from lung cancer patients (Figure 5D,E). The MCA results indicated that ctDNA samples from patient #2 tested positive for the EGFR L858R mutation, while the other two samples showed no presence of these seven mutations (Figure 5E). In order to validate these findings, NGS analysis was carried out on the tissue samples obtained from these patients, showing complete agreement with the multiplexed DMBA MCA results (Figure 5D). Mutations identified through NGS, which were not encompassed by the multiplexed DMBA MCA, are shaded in gray.

## DISCUSSION

Identification of low-abundance mutations in patients' blood posed a challenge due to excessive ctDNA fragmentation and interference from abundant wild-type DNA. Current qPCR methods are constrained by limited sensitivity, low multiplexing capabilities, and the need for template-specific and costly fluorescence probes.<sup>8,9,19,22,23</sup> Droplet digital PCR (ddPCR) enables absolute quantification of mutations by partitioning DNA samples into thousands to millions of droplets.<sup>36,37</sup> CRISPR-based methods have successfully detected mutations at VAFs below 0.01% by combining amplification and CRISPR detection.<sup>38,39</sup> However, ddPCR requires specialized instruments and has limited multiplexing capabilities. Similarly, CRISPR-based approaches are constrained by low multiplicity and the need for specific crRNA, Cas proteins, and an amplification step, leading to increased costs, complexity, and the risk of contamination through tube openings. MeltArray, the highly multiplexed technique coupled with melting curve analysis (MCA), is restricted to detecting mutations with Variant Allele Frequencies (VAFs) of either 5%

or 10%.<sup>32</sup> NGS has the capability to identify low-frequency variants through increased sequencing depth, as demonstrated by methods like CAPP-Seq<sup>13</sup> and Signatera.<sup>15</sup> However, challenges persist due to the expensive nature, intricate library preparation, and extended duration of these techniques. In this study, the new DMBA strategy exhibited advantages such as improved sensitivity, shorter amplicon lengths, and enhanced multiplicity. Its cost-effectiveness was enhanced by eliminating the need for specific fluorescence probes and any modified oligonucleotides. Moreover, the absence of a tube-opening step added simplicity and minimized the PCR contamination. The comparisons of these approaches are summarized in Table 1.

Due to the unique reaction mechanism, DMBA qPCR successfully detected four mutation targets at VAF of 0.01% using a universal Taqman probe with amplicons ranging from 67 to 83 bp. Single-plex DMBA MCA also achieved a variant detection sensitivity of 0.03% or 0.1% VAFs. Further, the multiplexed DMBA MCA successfully identified seven variants at VAFs levels of 0.1–0.5% using three universal fluorescence probes. Detection sensitivity can be increased to higher levels by employing oligonucleotides modified with LNA or PNA to enhance the affinity between DNA strands. To prevent melting peaks of wild-type DNA in DMBA MCA, inhibition of wild-type DNA amplification should be more efficient than in DMBA qPCR. As a result, the amplification of mutant DNA in DMBA MCA may be slightly hindered, providing a partial explanation for the increased sensitivity of DMBA qPCR in detecting mutations at lower VAFs compared to DMBA MCA.

The achievement of optimal reaction performance necessitated precise adjustments of the sequence and concentration of both MBs and mutant primers. In this study, we developed a multiplexed DMBA MCA capable of identifying seven mutations. With the utilization of four probes emitting distinct fluorescence and resulting in four unique melting peaks, a minimum of 16 targets can theoretically be distinguished in a single tube of DMBA MCA. Our future research will focus on diversifying the variety of targets detectable within DMBA MCA to 16 or more. However, increasing the multiplicity and reaction complexity could potentially compromise detection sensitivity. Therefore, achieving a balance between the two was crucial. This study involved the analysis of only three plasma samples using DMBA MCA with the matched tumor tissues analyzed using NGS. The validation of DMBA MCA's performance requires the development of a larger cohort with various confirmed mutation profiles, which is planned for future research. The effectiveness of DMBA on sequences with a high or low GC content was not investigated in this work. Although our method did not show a preference for either high- or low-GC sequences, it is still crucial to evaluate its

performance on these particular sequences prior to widespread implementation.

## ■ ASSOCIATED CONTENT

### SI Supporting Information

The Supporting Information is available free of charge at <https://pubs.acs.org/doi/10.1021/acs.analchem.5c04894>.

Amplification traces of amplifying BRAF V600E variant using mediator blocker (MB) of different amounts; melting curves for PIK3CA H1047R using mediator blockers at different amounts and lengths; detection of mutant DNA at variant allele frequencies (VAFs) of 0.1%, 0.3%, or 0.5% for all seven mutations through multiplexed DMBA MCA (PDF)

Information of gene-specific primers, blockers, and probes (XLSX)

## ■ AUTHOR INFORMATION

### Corresponding Authors

**Bingbing Wei** – Department of Urology, The Affiliated Wuxi People's Hospital of Nanjing Medical University, Wuxi People's Hospital, Wuxi Medical Center, Nanjing Medical University, Wuxi 214023, China; Email: [urowbb@njmu.edu.cn](mailto:urowbb@njmu.edu.cn)

**Lei Wang** – Department of Radiation Oncology, Lianyungang Clinical College of Nanjing Medical University (The First People's Hospital of Lianyungang), The First Affiliated Hospital of Kangda College of Nanjing Medical University, Lianyungang 222002, China; Email: [doctorwangl@163.com](mailto:doctorwangl@163.com)

**Zhaocheng Liu** – Department of Laboratory Medicine, The Affiliated Wuxi People's Hospital of Nanjing Medical University, Wuxi People's Hospital, Wuxi Medical Center, Nanjing Medical University, Wuxi 214023, China; [orcid.org/0009-0002-0992-4341](https://orcid.org/0009-0002-0992-4341); Email: [liuzhaocheng1130@163.com](mailto:liuzhaocheng1130@163.com)

### Authors

**Rui Zhang** – Department of Laboratory Medicine, The Affiliated Wuxi People's Hospital of Nanjing Medical University, Wuxi People's Hospital, Wuxi Medical Center, Nanjing Medical University, Wuxi 214023, China

**Zhenheng Pu** – Department of Laboratory Medicine, The Affiliated Wuxi People's Hospital of Nanjing Medical University, Wuxi People's Hospital, Wuxi Medical Center, Nanjing Medical University, Wuxi 214023, China

**Daxing Xu** – Department of Laboratory Medicine, The Affiliated Wuxi People's Hospital of Nanjing Medical University, Wuxi People's Hospital, Wuxi Medical Center, Nanjing Medical University, Wuxi 214023, China

**Ying Yin** – Department of Laboratory Medicine, The Affiliated Wuxi People's Hospital of Nanjing Medical University, Wuxi People's Hospital, Wuxi Medical Center, Nanjing Medical University, Wuxi 214023, China; [orcid.org/0000-0002-8367-1103](https://orcid.org/0000-0002-8367-1103)

Complete contact information is available at: <https://pubs.acs.org/doi/10.1021/acs.analchem.5c04894>

### Author Contributions

<sup>†</sup>R.Z. and Z.P. contributed equally to this work.

### Notes

The authors declare no competing financial interest.

## ■ ACKNOWLEDGMENTS

This work was supported by grants from the Natural Science Foundation of China (NSFC) (82402738), Wuxi Health Commission Youth Program (Q202311), Program of Wuxi Medical Center, Nanjing Medical University (WMCG202517, WMCG202416), The Talents of Double Hundred Talent Plan (BJ2023024), The Scientific and Technological Tackling (Basic Research) of TaihuLight (K20241018), The “333” Engineering Project Jiangsu Province ((2024) 3-2416), Cohort and Clinical Research Program of Wuxi Medical Center, Nanjing Medical University (WMCC202304), and Wuxi Medical Innovation Team (CXTD2021006).

## ■ REFERENCES

- (1) Ma, M.; Zhu, H.; Zhang, C.; Sun, X.; Gao, X.; Chen, G. *Ann. Transl. Med.* **2015**, *3*, 235.
- (2) Giménez-Capitán, A.; Bracht, J.; García, J. J.; Jordana-Ariza, N.; García, B.; Garzón, M.; Molina-Vila, M. A. *Clin. Chem.* **2021**, *67*, 554–563.
- (3) Yin, J.; Deng, J.; Wang, L.; Du, C.; Zhang, W.; Jiang, X. *Anal. Chem.* **2020**, *92*, 6968–6976.
- (4) Huiwen, C.; Kate, S.; Tatjana, J.; Bernard, T.; Joris Robert, V. *Extracell. Vesicles Circ. Nucleic Acids* **2022**, *3*, 216–234.
- (5) Riva, F.; Dronov, O. I.; Khomenko, D. I.; Huguet, F.; Louvet, C.; Mariani, P.; Bidard, F. C. *Mol. Oncol.* **2016**, *10*, 481–493.
- (6) Kurtz, D. M.; Soo, J.; Co Ting Keh, L.; Alig, S.; Chabon, J. J.; Sworder, B. J.; Alizadeh, A. A. *Nature biotechnology* **2021**, *39*, 1537–1547.
- (7) Qiu, B.; Guo, W.; Zhang, F.; Lv, F.; Ji, Y.; Peng, Y.; He, J. *Nat. Commun.* **2021**, *12*, 6770.
- (8) Newton, C. R.; Graham, A.; Heptinstall, L. E.; Powell, S. J.; Summers, C.; Kalsheker, N.; Markham, A. F. *Nucleic Acids Res.* **1989**, *17*, 2503–2516.
- (9) Wu, L. R.; Chen, S. X.; Wu, Y.; Patel, A. A.; Zhang, D. Y. *Nat. Biomed. Eng.* **2017**, *1*, 714–723.
- (10) Liu, Z.; Zhang, R.; Jiang, X.; Ji, L.; Sun, P.; Ji, Y.; Zou, J. *Anal. Chem.* **2023**, *95*, 12015–12023.
- (11) Park, J.; Abbas, N.; Park, Y.; Park, K. H.; Kim, Y. H.; Shin, S. *Sens. Actuators, B* **2022**, *355*, No. 131309.
- (12) Yang, Z.; Chen, W.; Wang, J.; Shi, M.; Zhang, R.; Dai, S.; Zhao, M. *Anal. Chem.* **2021**, *93*, 7086–7093.
- (13) Newman, A. M.; Bratman, S. V.; To, J.; Wynne, J. F.; Eclow, N. C. W.; Modlin, L. A.; Diehn, M. *Nat. Med. (N. Y., NY, U. S.)* **2014**, *20*, 548–554.
- (14) Schmitt, M. W.; Kennedy, S. R.; Salk, J. J.; Fox, E. J.; Hiatt, J. B.; Loeb, L. A. *Proc. Natl. Acad. Sci. U. S. A.* **2012**, *109*, 14508–14513.
- (15) Recio, F.; Scalise, C. B.; Loar, P.; Lumish, M.; Berman, T.; Peddada, A.; Holloway, R. W. *Gynecol. Oncol.* **2024**, *182*, 63–69.
- (16) Liu, G.; Ma, X.; Tang, Y.; Miao, P. *Analyst* **2020**, *145*, 1174–1178.
- (17) Chai, H.; Tang, Y.; Guo, Z.; Miao, P. *Anal. Chem.* **2022**, *94*, 2779–2784.
- (18) Wang, H.-F.; Ma, R.-N.; Sun, F.; Jia, L.-P.; Zhang, W.; Shang, L.; Wang, H.-S. *Biosens. Bioelectron.* **2018**, *122*, 224–230.
- (19) Oliveira, B. B.; Costa, B.; Morão, B.; Faías, S.; Veigas, B.; Pereira, L. P.; Baptista, P. V. *Anal. Bioanal. Chem.* **2023**, *415*, 2849–2863.
- (20) Morlan, J.; Baker, J.; Sinicropi, D. *PLoS One* **2009**, *4*, e4584–e4584.
- (21) Qu, S.; Liu, L.; Gan, S.; Feng, H.; Zhao, J.; Zhao, J.; Huang, J. *Clin. Biochem.* **2016**, *49*, 287–291.
- (22) Zhang, K.; Rodriguez, L.; Cheng, L. Y.; Wang, M.; Zhang, D. Y. *Anal. Chem.* **2022**, *94*, 934–943.
- (23) Yao, J.; Zhang, Z.; Huang, X.; Guo, Y. *Biosens. Bioelectron.* **2022**, *207*, No. 114138.
- (24) Kim, Y.-T.; Kim, J. W.; Kim, S. K.; Joe, G. H.; Hong, I. S. *Chembiochem* **2015**, *16*, 209–213.

- (25) Zuo, Z.; Chen, S. S.; Chandra, P. K.; Galbincea, J. M.; Soape, M.; Doan, S.; Luthra, R. *Mod. Pathol.* **2009**, *22*, 1023–1031.
- (26) How-Kit, A.; Lebbé, C.; Bousard, A.; Daunay, A.; Mazaleyrat, N.; Daviaud, C.; Tost, J. *Anal. Bioanal. Chem.* **2014**, *406*, 5513–5520.
- (27) Liu, Z.; Li, X.; Zhang, R.; Ji, L.; Gong, L.; Ji, Y.; Zou, J. *Anal. Bioanal. Chem.* **2023**, *415*, 6537–6549.
- (28) Mouliere, F.; Robert, B.; Arnau Peyrotte, E.; Del Rio, M.; Ychou, M.; Molina, F.; Thierry, A. R. *PLoS One* **2011**, *6*, No. e23418.
- (29) Zvereva, M.; Roberti, G.; Durand, G.; Voegelé, C.; Nguyen, M. D.; Delhomme, T. M.; Le Calvez-Kelm, F. *EBioMedicine* **2020**, *55*, No. 102462.
- (30) Huang, Q.; Zheng, L.; Zhu, Y.; Zhang, J.; Wen, H.; Huang, J.; Li, Q. *PLoS One* **2011**, *6*, No. e16033.
- (31) Chen, W.; Zhang, K.; Huang, F.; Zhao, L.; Waldren, G. C.; Jiang, Q.; Zhang, J. X. *Nucleic Acids Res.* **2024**, *52*, e81.
- (32) Huang, Q.; Chen, D.; Du, C.; Liu, Q.; Lin, S.; Liang, L.; Li, Q. *Proc. Natl. Acad. Sci. U. S. A.* **2022**, *119*, No. e2110672119.
- (33) Liu, Z.; Zhang, R.; Zhang, H.; Jing, L.; Yin, Y.; Jiang, X.; Li, K. *Sens. Actuators, B* **2024**, *418*, No. 136288.
- (34) Wang, M.; Huang, X.; Li, X.; Guo, Q.; Xu, W.; Zhao, M.; Lou, J. *Scand. J. Clin. Lab. Invest.* **2021**, *81*, 276–281.
- (35) Liu, W.; Wang, C.; Pan, F.; Shao, J.; Cui, Y.; Han, D.; Zhang, H. *Pathogens* **2023**, *12*, 719.
- (36) Yang, K.; Li, J.; Zhao, J.; Ren, P.; Wang, Z.; Wei, B.; Guo, Y. *Anal. Chem.* **2018**, *90*, 11203–11209.
- (37) Henriksen, T. V.; Drue, S. O.; Frydendahl, A.; Demuth, C.; Rasmussen, M. H.; Reinert, T.; Andersen, C. L. *Clin. Chem.* **2022**, *68*, 657–667.
- (38) Chen, K.; Dai, L.; Zhao, J.; Deng, M.; Song, L.; Bai, D.; Li, J. *Talanta* **2023**, *261*, No. 124674.
- (39) Liu, Z.; Xu, J.; Huang, S.; Dai, W.; Zhang, W.; Li, L.; Wu, T. *Biosens. Bioelectron.* **2024**, *247*, No. 115936.



CAS BIOFINDER DISCOVERY PLATFORM™

# PRECISION DATA FOR FASTER DRUG DISCOVERY

CAS BioFinder helps you identify  
targets, biomarkers, and pathways

Unlock insights

**CAS**  
A division of the  
American Chemical Society